AD-A139 579 RANGE-DOPPLER MOVING TARGET INDICATOR (MTI) ANALYSIS AND ASSESSMENT(U) NAVAL RESEARCH LAB WASHINGTON DC F F KRETSCHMER ET AL. 20 MAR 84 NRL-8789 1/1

UNCLASSIFIED F/G 17/9 NL

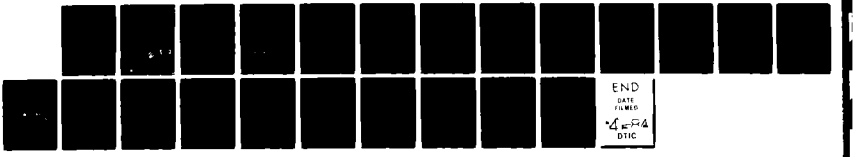

END
DATE FILMED
4-84
DTIC

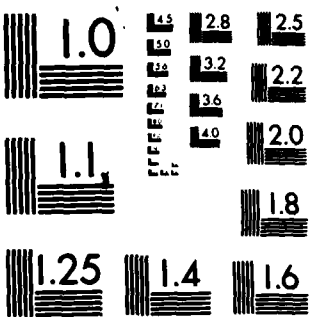

NRL Report 8789

Range-Doppler Coupled Moving Target Indicator (MTI) Analysis and Assessment

FRANK F. KRETSCHMER, JR., BERNARD L. LEWIS, AND FENG-LING C. LIN

Target Characteristics Branch
Radar Division

March 20, 1984

NAVAL RESEARCH LABORATORY
Washington, D.C.

SECURITY CLASSIFICATION OF THIS PAGE (When Data Entered)

REPORT DOCUMENTATION PAGE	READ INSTRUCTIONS BEFORE COMPLETING FORM
1. REPORT NUMBER: NRL Report 8789	2. GOVT ACCESSION NO.: AD-A139 529
3. RECIPIENT'S CATALOG NUMBER:	
4. TITLE (and Subtitle): RANGE-DOPPLER COUPLED MOVING TARGET INDICATOR (MTI) ANALYSIS AND ASSESSMENT	5. TYPE OF REPORT & PERIOD COVERED: Interim report on one phase of a continuing NRL problem.
	6. PERFORMING ORG. REPORT NUMBER:
7. AUTHOR(s): Frank F. Kretschmer, Jr., Bernard L. Lewis, and Feng-ling C. Lin	8. CONTRACT OR GRANT NUMBER(s):
9. PERFORMING ORGANIZATION NAME AND ADDRESS: Naval Research Laboratory, Washington, DC 20375	10. PROGRAM ELEMENT, PROJECT, TASK AREA & WORK UNIT NUMBERS: 62712N, SF12-131-691, 53-1810-0-0
11. CONTROLLING OFFICE NAME AND ADDRESS: Naval Sea Systems Command, Washington, DC 20362	12. REPORT DATE: March 20, 1984
	13. NUMBER OF PAGES: 20
14. MONITORING AGENCY NAME & ADDRESS(if different from Controlling Office)	15. SECURITY CLASS. (of this report): UNCLASSIFIED
	15a. DECLASSIFICATION/DOWNGRADING SCHEDULE:

16. DISTRIBUTION STATEMENT (of this Report)

Approved for public release; distribution unlimited.

17. DISTRIBUTION STATEMENT (of the abstract entered in Block 20, if different from Report)

18. SUPPLEMENTARY NOTES

19. KEY WORDS (Continue on reverse side if necessary and identify by block number)

Radar
Moving target indicator (MTI)
Pulse compression
Signal processing

20. ABSTRACT (Continue on reverse side if necessary and identify by block number)

The concept of a new moving target indicator (MTI) based on the range-doppler coupling properties of chirp, step-chirp, and certain polyphase codes is discussed. The principal feature of the range-doppler coupled MTI is that target blind speeds are eliminated. The polyphase codes must be symmetric for proper operation in a range-doppler coupled MTI. The performance of this MTI is evaluated, and its limitations are identified.

DD FORM 1 JAN 73 1473 EDITION OF 1 NOV 65 IS OBSOLETE
S/N 0102-014-6601

SECURITY CLASSIFICATION OF THIS PAGE (When Data Entered)

CONTENTS

RANGE-DOPPLER COUPLED MOVING TARGET INDICATOR (MTI) ANALYSIS AND ASSESSMENT

INTRODUCTION

In conventional long range search radars, the pulse repetition frequency (PRF) is such that unambiguous range information is obtained. However, at typical search radar transmit frequencies, the PRF is insufficient to prevent aliasing of the target's doppler spectrum. The consequence of this is that the velocity of the target is ambiguous and, more seriously, the target's doppler spectrum may fold over onto the spectrum of the clutter thereby precluding proper operation of the MTI which attempts to notch-out the clutter return. This undesirable situation is usually handled by consecutively transmitting slightly different constant PRF pulse trains or by transmitting a pulse-to-pulse staggered PRF.

Although transmitting pulse trains at different PRFs is generally simpler in terms of the MTI design and implementation, it tends to be more wasteful of pulses than the staggered-pulse MTI. However, a limitation of the staggered-pulse MTI is that ambiguous range clutter will not properly cancel. On the other hand, the multiple-pulse train MTI can perform properly in the presence of ambiguous range clutter if additional filler pulses are used to stabilize the ambiguous range clutter. However, in this case, a magnetron transmitter cannot be used since coherence is required on a pulse-to-pulse basis.

NRL Report 8592 [1] presents a different technique which eliminates blind speeds in an MTI resulting from targets whose doppler is a multiple of the PRF. This technique makes use of the well-known range-doppler coupling (RDC) which occurs with a frequency-swept waveform such as the chirp or the stepchirp waveform.

This report (8789) also reviews the underlying concepts and include the results of additional detailed analysis of the RDC MTI. The use of polyphase codes is described, and the applications and limitations of the technique are discussed.

RANGE-DOPPLER COUPLED MTI CONCEPT

Figure 1 depicts a simplified ambiguity diagram for a chirp waveform. The ordinate corresponds to the doppler shift of the received signal, while the abscissa represents time referenced to a value of zero for the nominal round-trip time delay of a point target. Figure 1 shows the trajectory of the peak response at the output of a matched filter for different doppler-shifted receive signals. For the upchirp signal denoted by the solid line, a doppler shift of f_d Hz results in a compressed pulse peak which is delayed by τ from the true round-trip propagation time of the radar signal. For a compressed downchirp radar signal, represented by the dashed line in Fig. 1, the same doppler shift causes the output signal to compress τ s ahead of the nominal time. This provides the basis for the RDC MTI since two consecutive pulses can be transmitted like a normal MTI except that one pulse is an upchirp signal and the other is a downchirp signal. By separately compressing each of the pulses (Fig. 2) and subtracting the signals noncoherently (or coherently), the resultant output signals will cancel completely only if the input signals are not doppler shifted. For doppler-shifted returns, the compressed signals will not cancel completely since they are displaced from each other and will appear, as shown in Fig. 2, when the pulses are separated by more than a compressed pulse width.

Manuscript approved October 17, 1983.

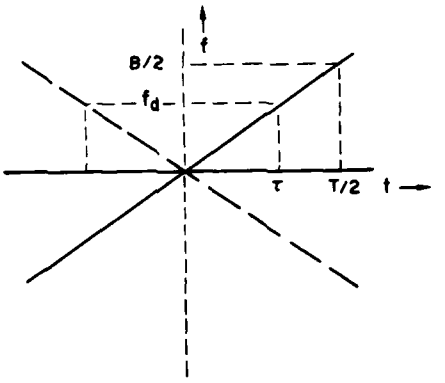

Fig. 1 — Range-doppler coupling

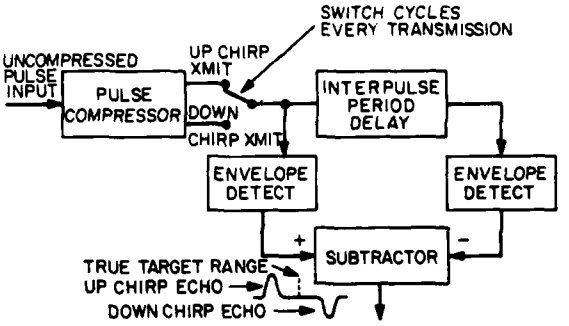

Fig. 2 — Two-pulse range-doppler coupled MTI (*noncoherent*) and response to incoming target

Figure 3 shows the amplitude of the resultant pulse, or pulses when they become separate, at the output of the subtracter in Fig. 2 for idealized bandlimited compressed pulses. For a velocity higher than V_m, the response is flat so that there are no blind velocity targets. Note that clutter signals having a small velocity will be attenuated by the RDC MTI filtering. The velocity V_m is next derived by referring to the upchirp response (solid line) in Fig. 1. The slope of this line is

$$k = B/T, \tag{1}$$

where B is the signal bandwidth and T is the uncompressed pulse length; thus,

$$f_d = k\tau \tag{2}$$

from which

$$\tau = f_d/k = (f_d/B)\,T. \tag{3}$$

The number of range cells ΔR corresponding to a delay of τ s is then given by

$$\Delta R = \tau B = (f_d/B)\rho = f_d T, \tag{4}$$

where ρ is the pulse compression ratio TB. To resolve the compressed pulses after subtraction, we assume that they are separated by a pulse width or that each pulse is shifted oppositely in time by $\tau = 1/2B$. Therefore,

$$\Delta R = \tau B = 1/2 = f_d T = 2(V_m/\lambda)\,T, \tag{5}$$

and

$$V_m = \lambda/(4T) = C/(4Tf_0). \tag{6}$$

From the relation

$$V_m = C/(4Tf_0),$$

V_m is decreased by increasing T and/or f_0. For example, for $V_m = 300$ m/s, we require that at X-band $T = 25\ \mu$ and at S-band $T = 75\ \mu$s. Note that T can also be increased without changing the bandwidth or duty cycle by leaving spaces in the transmitted waveform. This is more readily achievable with the polyphase coding which is described subsequently.

Figure 3 shows the slope of the response curve in the notch region is $1/V_m$. The amplitude response A may therefore be written as

$$A = V/V_m.$$

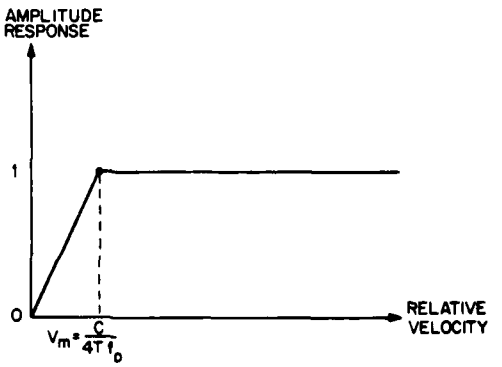

Fig. 3 — Response of noncoherent range-doppler coupled MTI

In this region, the ratio of amplitude response is the same as the ratio of the relative velocities. Thus a doubling of the relative velocity results in a 6-dB increase in peak signal power.

Figure 4 shows the response curve or the coherent RDC MTI using idealized pulses for an interpulse period T_I equal to 10 times the uncompressed pulse width T. In this case, the phase of the target returns from pulse to pulse must be taken into account. The first peak of the cyclic response in Fig. 4 occurs at a velocity V_1 when there is a π phase shift between successive pulses as is the case with the normal coherent MTI canceler. When there is a 2π phase shift between successive pulses, the normal MTI response goes to zero and this corresponds to the first blind velocity. For the RDC MTI, however, the response does not go to zero since the compressed pulses have moved apart due to range-doppler coupling before subtraction. A peak in the cyclic response occurs at odd multiples of π phase shift from pulse to pulse. When a π phase shift occurs within the uncompressed pulse, the compressed pulses are separated by one pulse width and the response is at the peak. This is evident from Eq. (5) where we had

$$f_d T = 1/2$$

so that total phase shift across the uncompressed pulse $\Delta\phi$ is

$$\Delta\phi = 2\pi f_d T = \pi.$$

The number of cyclic peaks occurring in a coherent RDC response curve as shown in Fig. 4 is then given by one-half of the ratio of T_I to the uncompressed pulse length. The lower part of the cyclic swing is the same as the noncoherent response shown in Fig. 3. Also the upper part of the cyclic swing is bounded by the upper dashed line in Fig. 4 which is the symmetrical counterpart of the lower bound. This indicates that the target response of the coherent RDC MTI is equal to or larger than for the noncoherent MTI when $V < V_m$, and for $V > V_m$ the two are the same.

The noncoherent RDC MTI allows determination of the velocity direction by noting the signs of the pulse pair after the subtractor in Fig. 2. Also, the noncoherent RDC MTI does not require a clutter background for proper operation as the normal noncoherent MTI does. The normal noncoherent MTI tends to cancel targets in the clear if strong clutter is not present. The RDC MTI case permits detection of higher velocity targets because of the time separation of the output pulses due to range-doppler coupling.

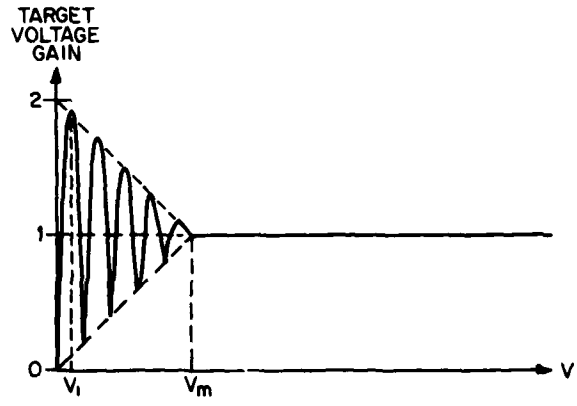

Fig. 4 — Response of coherent 2-pulse range-doppler coupled MTI with $T/T_l = 10$

PERFORMANCE ANALYSIS

Chirp and Polyphase Code Response Curves

Figure 5 shows the computer-simulated result of noncoherently subtracting two compressed Hanning-weighted chirp pulses having a total separation of approximately 0.1 and 0.6 of a pulse width. Figure 6 shows a plot of the peak signal after noncoherent subtraction of the Hanning-weighted chirp signals.

Since the polyphase codes recently investigated by the authors [2] also exhibit range-doppler coupling properties, they can also be used in an RDC MTI. Figure 7 shows a compressed pulse for a 100-element ($\rho = 100$) P2 polyphase code [2] where the sample numbers correspond to range resolution cells. Figure 8 shows the results on an amplitude scale of noncoherently subtracting an upsweep and a downsweep 100-element P2 code after compression for two different target velocities. The peak amplitude of the compressed pulses for zero doppler is 100 prior to subtraction. The downsweep version of the P2 code or any other polyphase code is obtained by taking the conjugate (negative) phases of the upsweep or normal version of the polyphase codes. Figure 9 shows the RDC MTI response curve for the 100-element P2 code for the coherent and noncoherent cases. The cyclic minima for the coherent case do not equal the noncoherent case as they do for a chirp signal. Figure 10 shows an approximation to a chirp signal where we have used a polyphase code obtained by using 2ρ phase samples (rather than ρ) taken from the quadratic phase characteristic of a chirp signal at twice the Nyquist rate. The compressed waveform for this case has the same peak sidelobes and behaves approximately the same as the chirp waveform.

The polyphase codes differ in several other respects from the chirp signals. Figure 9 shows that the polyphase code response is full amplitude (100 units) for a normalized doppler shift of approximately 0.01 rather than 0.005 for the simulated chirp signal shown in Fig. 10. This is due to the peak response of the polyphase code splitting into two adjacent cells with a reduced amplitude for a doppler shift of 0.005. At a doppler shift of 0.01, there is one peak at full amplitude. This corresponds, in general, to a total range separation between the upsweep and downsweep versions of the polyphase code being two range cells rather than one range cell for the chirp signal. Also, for higher doppler velocities, Fig. 9 shows the amplitude of the polyphase codes cycles for doppler shifts higher than 0.01. This is a property of the polyphase codes [2] which does not occur with the chirp signal. The cycling shown in Fig. 10 beyond the normalized doppler frequency of 0.01 is due to using a polyphase code in approximating a chirp signal.

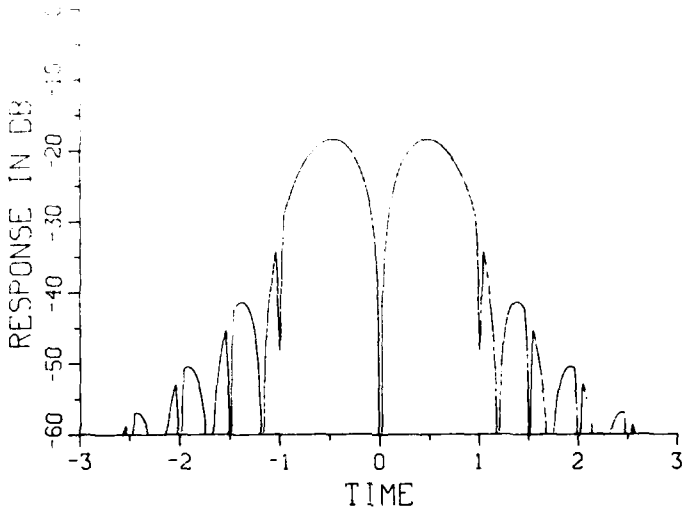

(a)

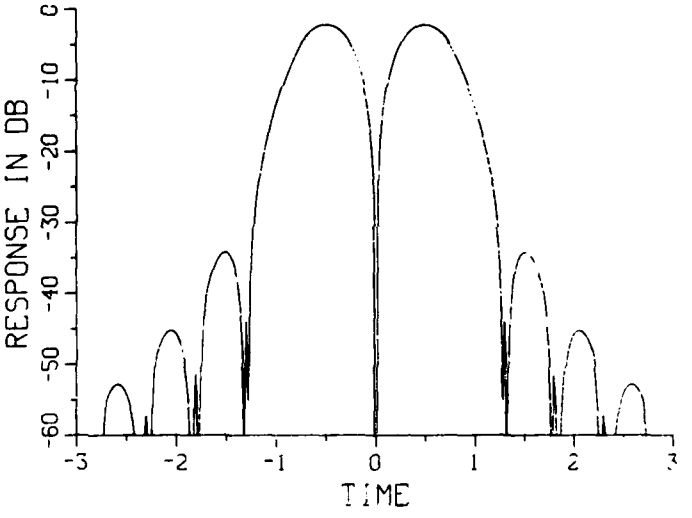

(b)

Fig. 5 — Noncoherent subtraction of two range-doppler coupled Hanning-weighted chirp pulses. Time scale is in units of a pulse width. (a) Separated by approximately 0.1 pulse width (b) Separated by 0.6 pulse width

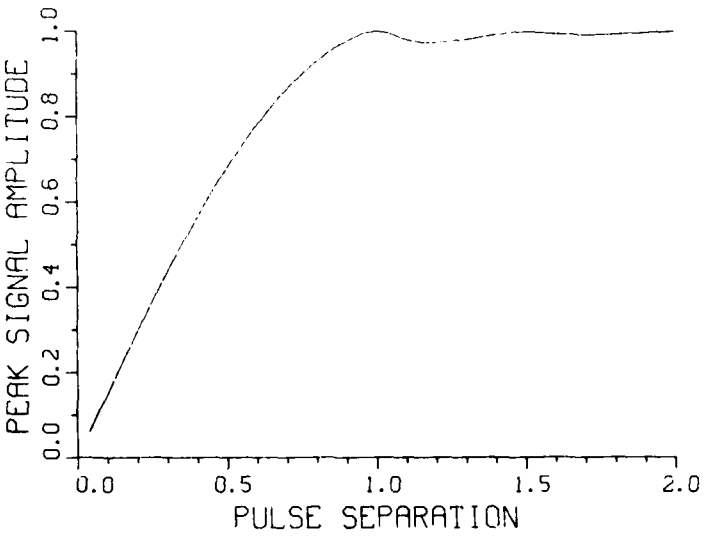

Fig. 6 — Peak response of noncoherent range-doppler coupled MTI using Hanning-weighted chirp signals. Pulse separation is in units of a pulse width

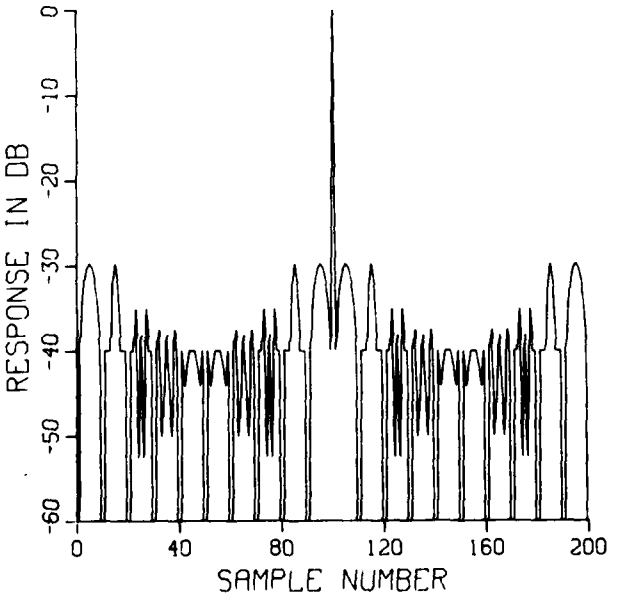

Fig. 7 — Compressed 100-element P2 polyphase code

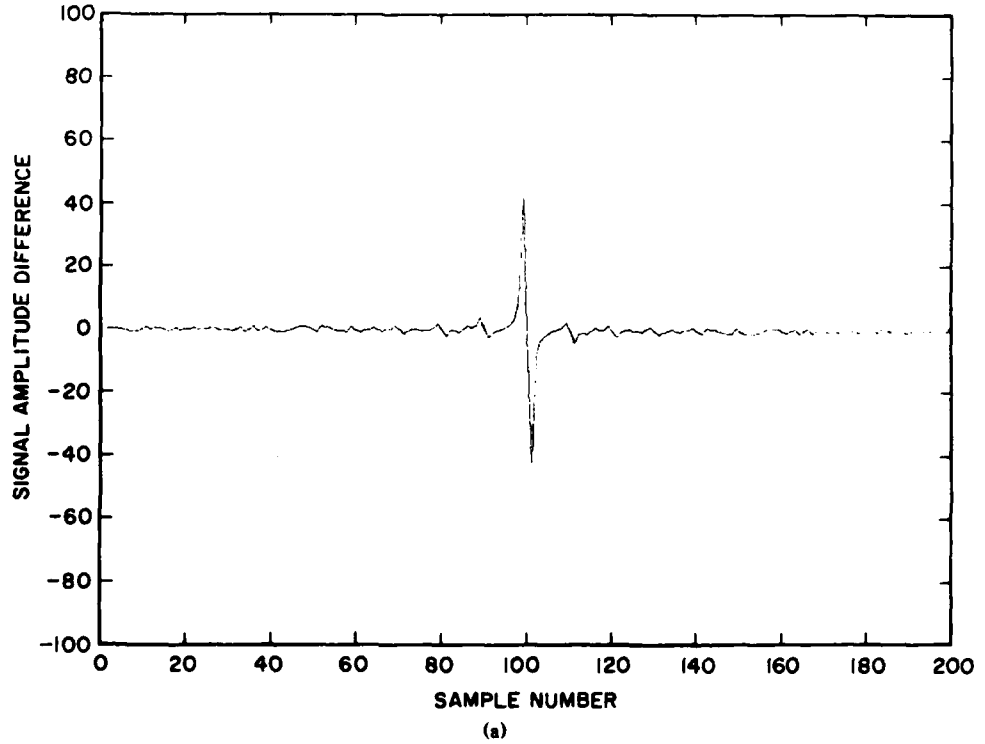

(a)

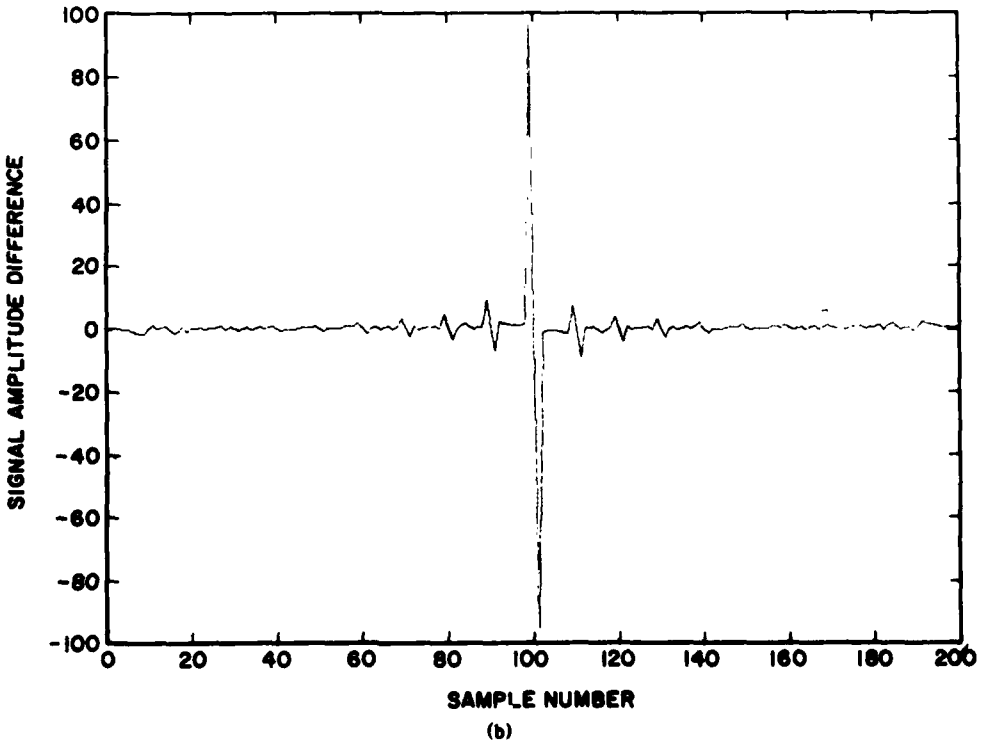

(b)

Fig. 8 — Target response for 2-pulse range-doppler coupled MTI using a 100-element P2 polyphase coded waveform (a) Normalized target doppler is 0.005 B (b) Normalized target doppler is 0.01 B

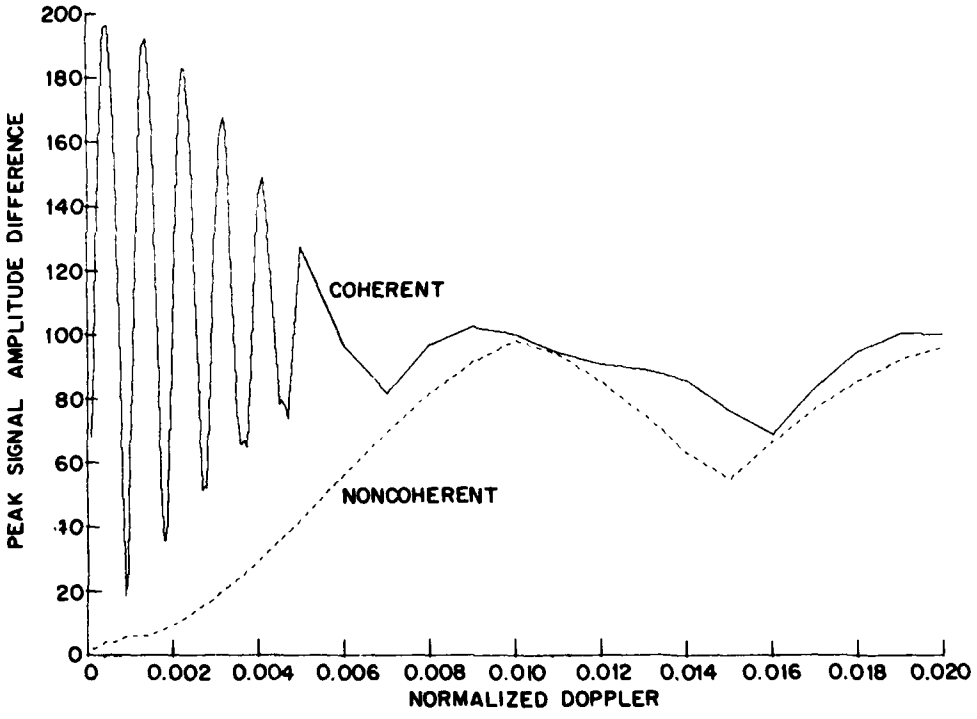

Fig. 9 — Response of a range-doppler coupled MTI for a doppler-shifted target using a 100-element P2 polyphase coded waveform

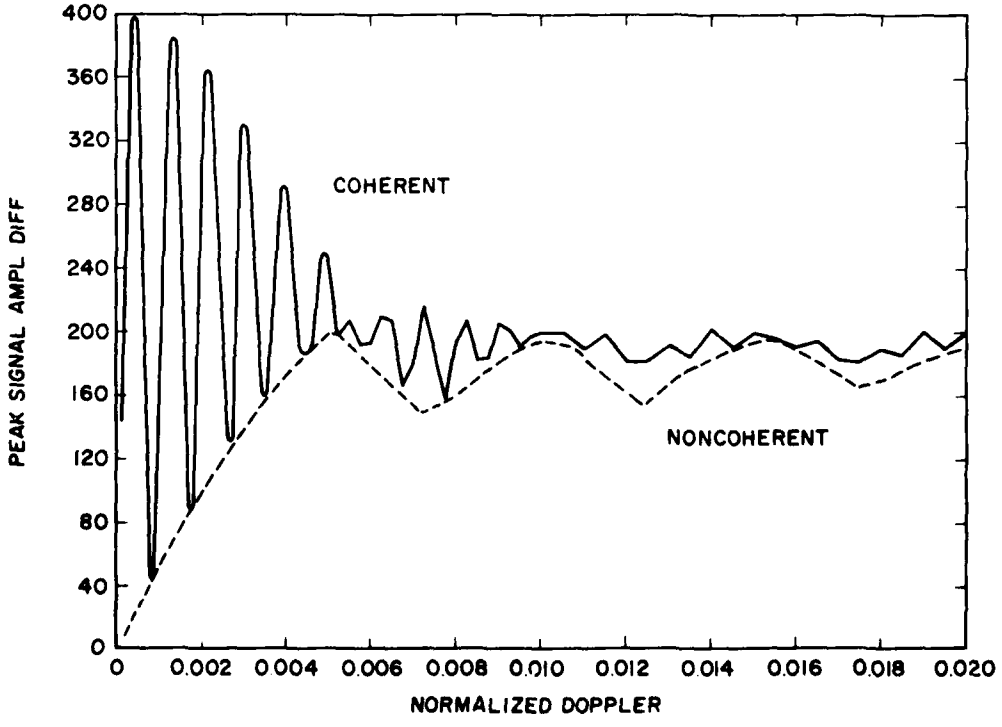

Fig. 10 — Response for a range-doppler coupled MTI for a chirp signal approximated by a 200-element polyphase code

Evaluation of the RDC MTI Improvement Factor

An analysis was performed to determine the effect on the MTI cancellation ratio (CR) of the range-doppler coupling effect. This is summarized in the appendix of this report. The range-doppler coupling of the clutter for typical clutter spectral widths (assuming a Gaussian power spectral density function) had a negligible effect on the cancellation ratio. This is attributed to the transfer function of the range-doppler coupled MTI being approximately the same as the normal coherent or noncoherent MTI counterparts in the small doppler region near zero that is occupied by the clutter.

The average improvement factor I for a coherent MTI is computed from the relation

$$I = CR \cdot TE,$$

where TE denotes the average target gain or enhancement over the region of interest. Referring to Fig. 4, the target enhancement evaluated from 0 doppler to a doppler $F > F_m$ ($F_m = 2\ V_m/\lambda$) for the 2-pulse coherent RDC MTI using chirp signals can be determined from

$$TE = \frac{1}{F}\left[\int_0^{F_M} E^2(f)\,df + 1\right], \tag{7}$$

where

$$E(f) = [(1 - f/F_m)\sin \pi fT + 1].$$

Substituting for $E(f)$ in Eq. (7) results in

$$TE = \frac{1}{F}\Big[\int_0^{F_M} [(1 - 2f/F_m + f^2/F_m^2)\sin^2 \pi ft + 2(1 - f/F_m)\sin \pi fT + 1]\,df + 1\Big]. \tag{8}$$

This can be written as the sum of integrals which are in standard form. However, an approximate solution can be obtained by considering Fig. 4 and noting that by integrating over a large doppler region compared to F_m, TE approaches unity and represents a 3-dB loss in improvement factor relative to the normal MTI. For higher order cancelers, the loss is less. For polyphase codes, there is an additional loss due to the cycling of the resolved peak signals as previously discussed. However, in either case, the tradeoff is that the velocity response has been extended to prevent target blind speeds.

It was found in the simulations described in the appendix of this report that the noncoherent RDC MTI performed the same way relative to the coherent RDC MTI as it does for the normal MTI [3]. The improvement factors of the noncoherent and coherent RDC MTIs are the same for the two-pulse canceler but differ from the normal MTI as described in the preceding section. According to Ref. 3, the noncoherent MTI improvment factor degrades relative to the coherent MTI for binomial weighting as the number of pulses exceeds two.

Use of Polyphase Codes in Extended Clutter

A weighted P4 polyphase code was used in a 2-pulse RDC MTI simulation in which extended clutter having zero doppler was generated. It was assumed that the clutter power per range cell (or sample number) was unity and that the clutter had an independent Gaussian distribution from range cell to range cell.

Figure 11 shows the results of this simulation where the target doppler is such that it range-doppler couples one range cell and hence the target occupies two range cells at the output of the RDC MTI. However, as shown in Fig. 11, the clutter was only cancelled by approximately 20 dB; this is because the P4 code is not symmetrical about the center of the code. This in turn results in a

compressed pulse which is complex, and the upchirp and downchirp compressed pulses are not identical. Whereas the P2 is a symmetrical code, the unsymmetrical P1, P3, and P4 codes can be made symmetrical by shifting the initial sampling point one-half of a subpulse width in deriving these codes from the underlying phase characteristic. The symmetrical version of these codes is denoted by the prefixed letter P (for palindromic) such as the PP4 code. Figure 12 illustrates the derivation of the P4 and PP4 code phases from the sampled quadratic-phase characteristic of a linear chirp signal.

By using symmetrical polyphase codes, the compressed pulse is real and symmetrical, which results in identical upchirp and downchirp versions. For this case, the nonmoving extended clutter cancelled completely, provided the extended clutter is unambiguous in range (Figs. 13 and 14).

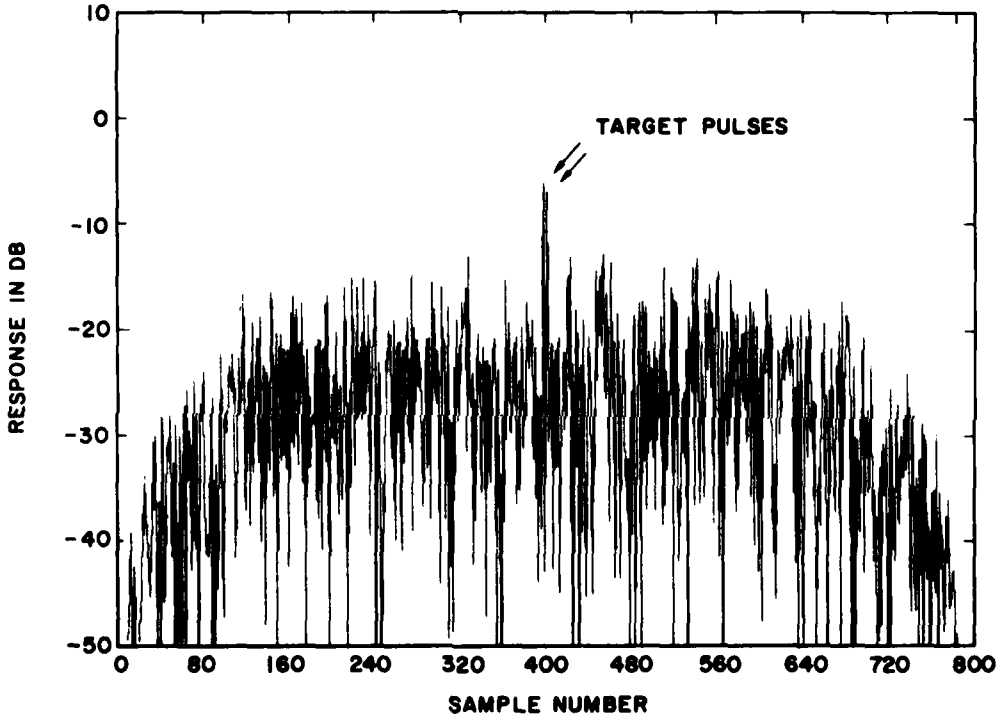

Fig. 11 — Simulated output of a 2-pulse range-doppler coupled MTI for a target embedded in zero velocity distributed clutter using a weighted P4 code. The target's normalized doppler is 0.01 B.

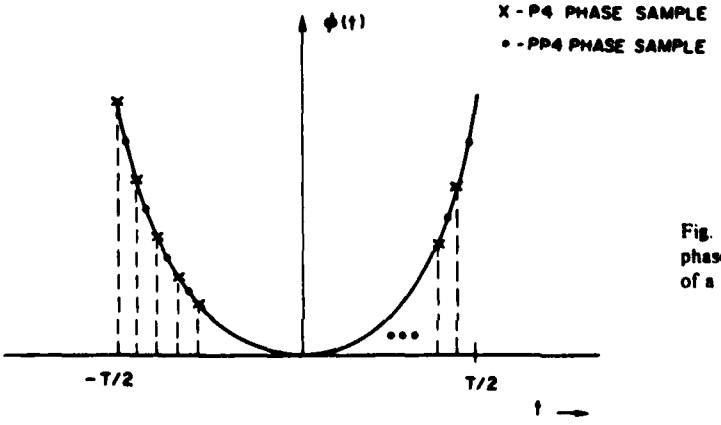

Fig. 12 — Derivation of P4 and PP4 polyphase code phases by sampling the quadratic phase characteristic of a chirp signal

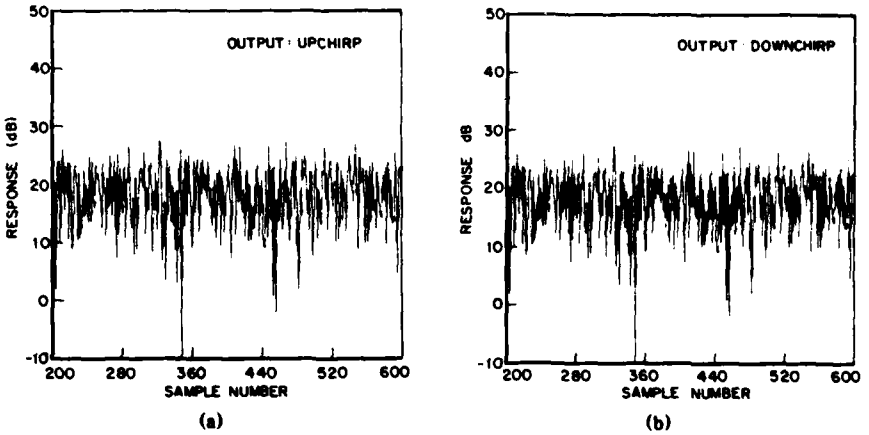

Fig. 13 — Output of the (a) upchirp and (b) downchirp pulse compressors for distributed clutter and a target using a 100 element PP4 code. Clutter-to-target ratio is 20 dB. Clutter doppler is zero and target doppler is 0.01 B.

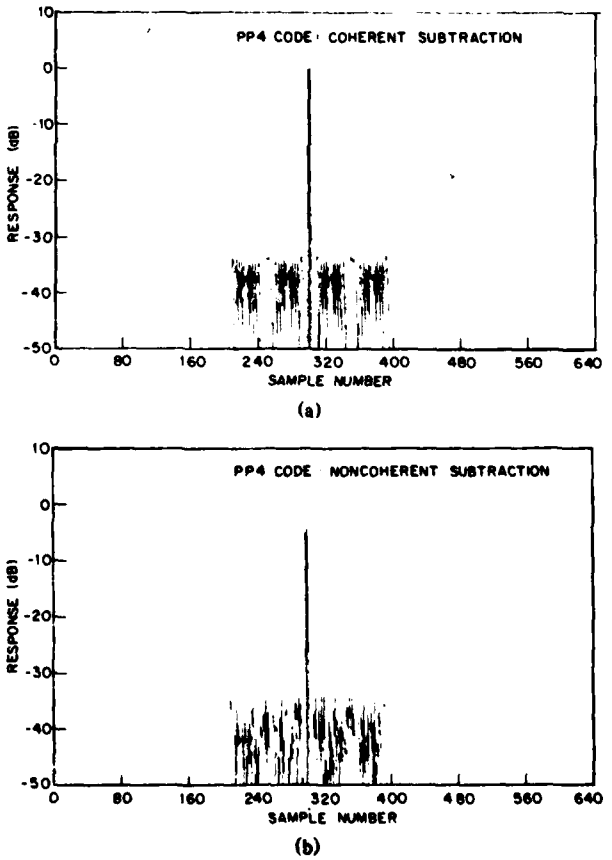

Fig. 14 — Output of range-doppler coupled MTI showing target alone (a) Coherent subtraction (b) Noncoherent subtraction

RANGE-AMBIGUOUS EXTENDED CLUTTER

Simulations were performed for ambiguous range-extended clutter. The upchirp and downchirp signals were assumed to be transmitted simultaneously for convenience as shown in Fig. 15. If the pulses were transmitted with a separation of τ s, the channel matched to the first transmitted pulse would be delayed by τ. The important result, however, is that range-ambiguous stationary clutter does not properly cancel. This is shown in Fig. 16 where 0 dB corresponds to the input clutter power level. This residue is attributed to the cross responses not cancelling, i.e., the response of the upchirp signal in the filter matched to the downchirp signal and vice versa. It is important to realize that for ambiguous range clutter, one cannot compress each upchirp or downchirp pulse separately as shown in Fig. 2 for unambiguous clutter. The cross responses have the same amplitudes, but unequal phases which are symmetrical about any constant phase angle of the input signal. Figure 17 shows the magnitude responses for the matched and mismatched channels For the special case of a zero-degree constant phase angle associated with the received waveform, the phases in the mismatched channels are conjugates of each other for a point target return. The fact that proper cancellation does not take place for ambiguous range returns places a performance limitation on the RDC MTI similar to that for a pulse-to-pulse staggered waveform used to remove blind speeds in a conventional MTI.

Although the RDC MTI does not work properly in range-ambiguous extended clutter, it may have applications in making velocity measurements on a target in the clear.

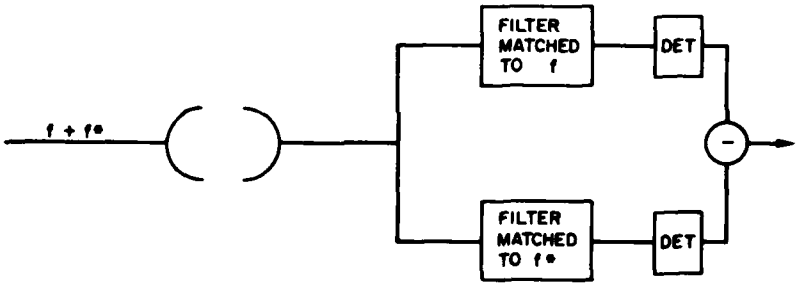

Fig. 15 — Range-doppler coupled MTI for ambiguous range case

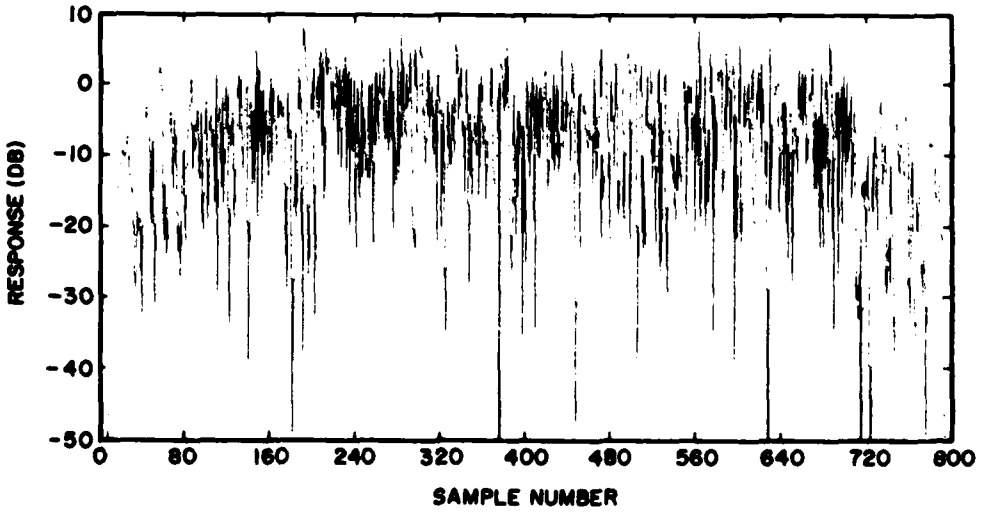

Fig. 16 — Range-doppler coupled MTI output for nonmoving distributed clutter

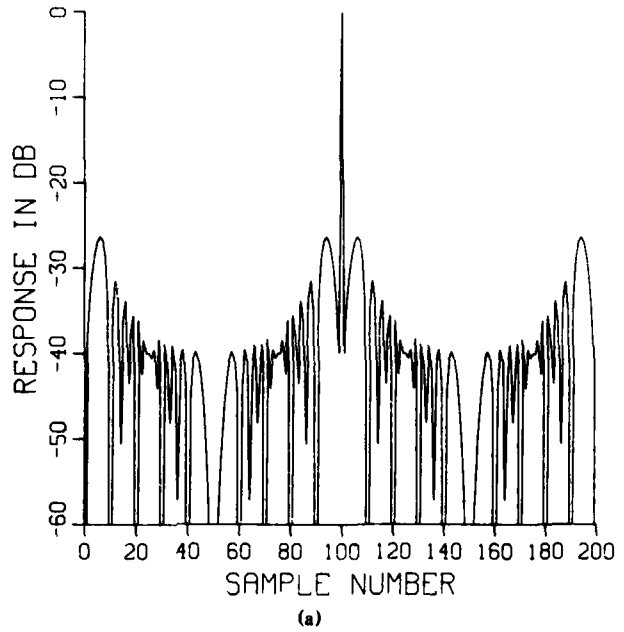

(a)

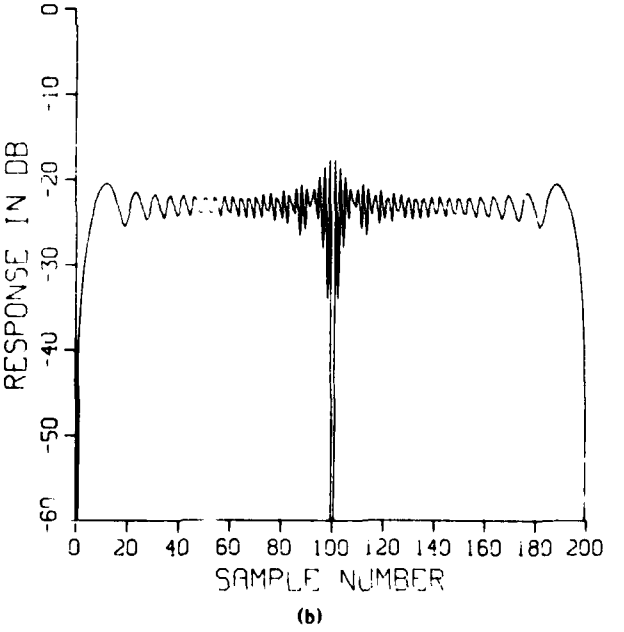

(b)

Fig. 17 — Outputs of range-doppler coupled MTI pulse compressors for 100-element PP4 code (a) Matched channel (b) Mismatched channel

SUMMARY AND CONCLUSIONS

The concept of a range doppler coupled MTI was presented where it was shown that target blind speeds could be prevented. It was shown that a relatively flat target response is obtained for targets having doppler velocities above V_m which corresponds to a range shift, due to range-doppler coupling, of 1/2 or 1 range cell depending on whether chirp signals or polyphase codes are used. V_m, in turn, was shown to be inversely proportional to the product of Tf_o, where T is the uncompressed pulse width and f_o is the transmit center frequency. For chirp signals, for example, with V_m = 300 m/s, we require T = 25 μs or 75 μs at X band and S band. At the lower frequencies, where the pulse length becomes larger, it is not necessary to transmit continuously for a time T. The overall transmission time T could consist of transmissions and spaces with the appropriate matched filtering. Note that an improvement in the target-to-clutter ratio is also achieved for target velocities less than V_m as long as the target velocity is larger than that of clutter. This means that the time duration T can be traded off.

The problem of multiple targets could cause some confusion in the coherent RDC MTI. However, there are several mitigating factors. In the previous example, a 600-m/s target would result in two pulses separated by only one range cell, and for Swerling I or Swerling III targets would have similar amplitudes which may be helpful in associating the pulses. For noncoherent RDC MTI either the positive or the negative pulses of the pulse pair from each target could be eliminated and then only one pulse would be associated with each target as in a regular MTI system using pulse compression.

It was shown that the range-doppler coupling effect of the clutter is negligible and that the RDC MTI has a cancellation ratio which is approximately the same as the normal MTI for both the coherent and noncoherent cases. However, the improvement factor, which consists of the cancellation ratio times the target enhancement factor, is less than the regular coherent or noncoherent MTI when averaging the target response over large doppler frequencies. This is mainly due to the RDC MTI target transfer function being approximately unity for a two-pulse canceler with resolved pulses at the RDC MTI output. Thus, for a two-pulse binomial weighting, the loss in target enhancement and also the resultant improvement factor is approximately 3 dB. However, one reduces the blind speed problem by using this technique. There also appears to be a loss associated with the staggered pulse MTI; however, we have not quantitatively analyzed this loss.

An advantage of the noncoherent RDC MTI over its normal noncoherent MTI counterpart is that it does not require the presence of clutter for proper operation. The normal noncoherent MTI tends to cancel targets in the clear unless strong clutter is present.

It was shown that, like the staggered pulse MTI, the RDC MTI does not work properly in range ambiguous extended clutter. It was also shown that for unambiguous extended clutter that the unsymmetrical polyphase codes could not be used since the compressed pulses for the unsymmetrical codes were complex and differed in phase between the upchirp and downchirp versions of the compressed codes. Symmetrical phase codes were derived which are suitable for use with the RDC MTI.

Although there is no reason to recommend using the RDC MTI in preference to the pulse-to-pulse staggered MTI for eliminating target blind speeds, the RDC MTI provides an alternate technique which may have other useful applications, such as providing velocity information on isolated targets in the clear.

REFERENCES

1. B. L. Lewis, F. F. Kretschmer, Jr., and F. C. Lin, "Range-Doppler-Coupled Moving Target Indicator," NRL Report 8592, June 1982.

2. F. F. Kretschmer, Jr., and B. L. Lewis, "Doppler Properties of Polyphase Coded Pulse Compression Waveforms," *IEEE Trans. Aerospace and Electronic Systems* **AES-19** (4), July 1983.

3. F. F. Kretschmer, Jr., F. C. Lin, and B. L. Lewis, " A Comparison of Noncoherent and Coherent MTI Improvement Factors," *IEEE Trans. Aerospace and Electronic Systems* **AES-19** (3) May 1983.

Appendix

Previous methods [A1] that were used to simulate coherent and noncoherent MTI performance were inappropriate for analyzing the RDC MTI. For this analysis, a different approach was taken. To assess the range-doppler coupling effects of the clutter, the narrowband Gaussian clutter spectrum shown in Fig. A1 was approximated by the discrete line spectra as shown in Fig. A2 [A2]. The voltage for this approximation is then given by

$$c(t) = \sum_{m=1}^{M} [2G(f_1 + m\Delta f)\Delta f]^{1/2} \cos [\,(\omega_1 + m\Delta\omega)\, t + \theta_m],$$

where θ_m is an independent and uniformly distributed phase term. We may also write $c(t)$ as

$$c(t) = x(t)\cos \omega_c t - y(t)\sin \omega_c t,$$

where

$$x(t) = \sum_{m=1}^{M} [2G(f_1 + m\Delta f)\Delta f]^{1/2} \cos [(\omega_m - \omega_c)t + \theta_m],$$

$$y(t) = \sum [2G(f_1 + m\Delta f)\Delta f]^{1/2} \sin [(\omega_m - \omega_c)t + \theta_m],$$

and

$\omega_m = \omega_1 + m\Delta\omega$, and ω_c = carrier frequency.

It may be shown that x(t) and y(t) have a Gaussian probability distribution [A2] as desired and that c(t) has the proper power density spectrum which in turn defines the underlying correlation function of the clutter. This approach allowed us to compute the effect of RDC by processing each spectral line separately.

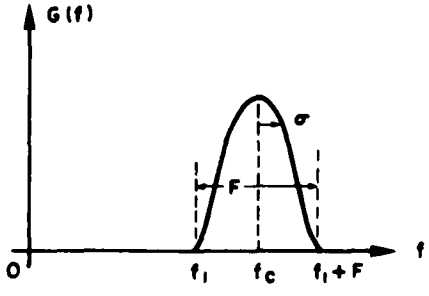

Fig. A1 — Narrowband Gaussian clutter spectrum

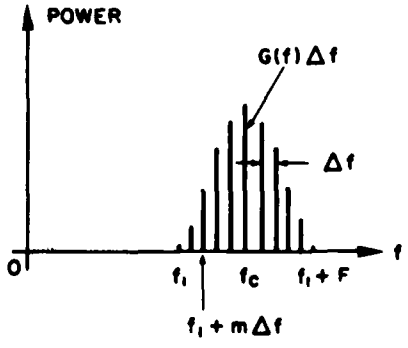

Fig. A2 — Discrete approximation to the narrowband spectrum

Simulations of the normal MTI were performed by using an analytical approach, a Monte Carlo simulation as described in Ref. A1, and the approach based on the approximated power spectrum as previously described; agreement was obtained. Approximately 11 spectral lines, and the average of approximately 500 sets of 11 random phases gave a good approximation.

Various Monte Carlo simulations were performed for the RDC MTI using the polyphase codes. In one simulation a target was embedded in clutter which appeared in four adjacent range cells and had

a C/T of 20 dB. Improvement factors were computed over several doppler regions of the response curve, such as shown in Fig. A3, by averaging the results over the specified doppler regions. In this simulation the range shifted target, due to RDC, competed with clutter. The simulation took into account the superposition of the reflections of an uncompressed PP4 code from the randomized clutter in the different range cells. The clutter was assumed to have a complex Gaussian probability distribution in each range cell and to be independent from cell to cell. Each spectral line of the approximated clutter spectrum gave rise to a doppler-shifted uncompressed pulse which was compressed and then processed according to the RDC MTI as in Fig. A4. The residue on a given trial was obtained from the sum of the residues from the individual spectral lines. This was repeated 500 times, using different phase distributions for the spectral lines for each range cell. In this simulation, we could account for the doppler shift of the clutter within the pulse, and hence, the RDC corresponding to each spectral line, or we could ignore it to determine the difference. In either case, the phase shift of the clutter, due to doppler, between two pulses separated by an interpulse period was taken into account.

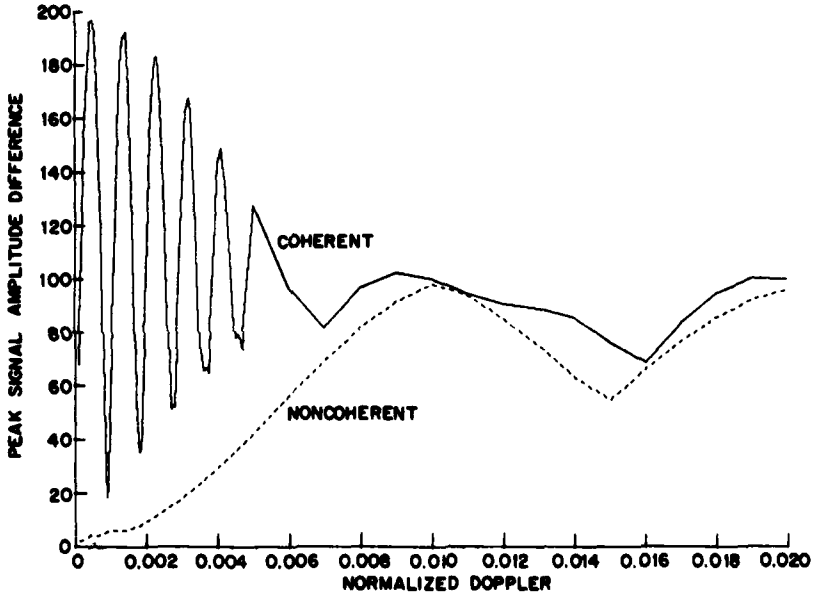

Fig. A3 — Response of a range-doppler coupled MTI for a doppler-shifted target using a 100-element P2 polyphase coded waveform

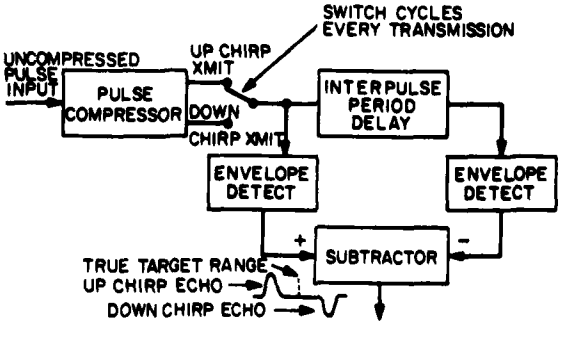

Fig. A4 — Two-pulse range-doppler coupled MTI (noncoherent) and response to incoming target

Table A1 summarizes these results for a two-pulse range-doppler coupled MTI using a 16-element PP4 code. Both the coherent and noncoherent cases were simulated. In this simulation, the ratio of the standard deviation of the Gaussian spectrum to the PRF was assumed to be 0.005. In Table A1, IPP = 1 means that the RDC effect on the clutter was included. IPP = 0 means that only the pulse-to-pulse phase shift of the clutter was taken into account. The improvement factor was computed for different regions of the target doppler. Table A1 shows the results for the improvement factor averaged over one PRF near 0 doppler and over the same interval near the corner frequency F_m corresponding to the velocity V_m.

Table A1 — Simulation of Clutter Attenuation (CA) and Improvement Factor (IMP) for RDC MTI using a 16-element PP4 Code at Different Target Doppler Frequencies

Target Doppler	IPP	Coherent		Noncoherent	
		CA	IMP	CA	IMP
Near 0.0	0	30.19	33.31	33.04	33.13
Near F_m	0	29.81	29.28	32.28	28.45
Near 0.0	1	30.35	33.45	33.03	33.01
Near F_m	1	29.93	29.25	32.71	28.98

For IPP = 0 the clutter attenuation and the improvement factor for the target averaged over one PRF interval of the MTI response near zero doppler is approximately the same as we obtained for the normal MTI for both the coherent and the noncoherent cases (see Table A1). It is seen that taking into account the RDC effect of the clutter (IPP = 1) had a negligible effect. This was also observed in other simulations that were performed.

Another result shown in Table A1 is that the clutter attenuation is the same, as it should be, for the target dopplers averaged over one PRF at zero frequency and at the corner frequency F_m. However, there is an approximate loss of 3 dB in the improvement factor for the coherent case at F_m due to the reduced average target response in this region. This is an expected result which can be deduced from the reponse curves, such as Fig. A5, and the fact that the clutter attenuation and the improve-

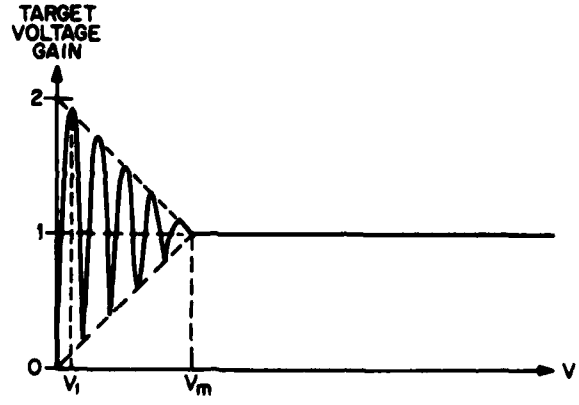

Fig. A5 — Response of coherent 2-pulse range-doppler coupled MTI with $T/T_i = 10$

ment factors were approximately the same as the normal coherent MTI (see Table A1). For the 2-pulse normal MTI, the target enhancement factor is theoretically 3 dB, and in Fig. A5 the response averaged over one PRF at $f = F_m$ is unity thereby representing a 3-dB reduction in the target enhancement and, hence, in the associated improvement factor.

REFERENCES

A1. F. F. Kretschmer, Jr., F. C. Lin, and B. L. Lewis, "A Comparison of Noncoherent and Coherent MTI Improvement Factors," *IEEE Trans., Aerospace and Electric Systems,* **AES-19**, No. 3, May 1983.

A2. M. Schwartz, "Information Transmission, Modulation and Noise," pp. 363-369, 2nd edition, McGraw-Hill, New York, 1970.


LMED